AUTOMOTIVE BLOWER DESIGN WITH INVERSE METHOD APPLIED ON WHEEL AND VOLUTE

Manuel HENNER[1], Youssef BEDDADI[1], Bruno DEMORY[1],
Mehrdad ZANGENEH[2]

[1] *Valeo Thermal Systems, 8 rue Louis Lormand, 78321 La Verrière France*

[2] *Department of Mechanical Engineering, University College London, London WC1E 7JE, UK*

SUMMARY

A method aimed to reduce the development time of an automotive blower is investigated. The objectives are to improve the efficiency, to reduce the losses and flow unsteadiness. Wheel and volute performances are analyzed on an existing geometry, and results are used to specify targets for a 3D inverse design method. Constraints on packaging and process complete the specifications. Better performances of the new wheel are further improved with the re-design of the volute with a 2D inverse design method for the design of the volute that can take account of circumferential variation in inflow velocity to the volute. Overall performance and detailed flow analysis are verified by numerical simulation and compared to the original design.

INTRODUCTION

Expectations in terms of energy efficiency, thermal and acoustic comfort are increasingly important in the automotive industry. The radial fan that is commonly used for the thermal management of the interior is particularly important because ventilation performance contributes to the well being of passengers. Performance targets are all the more challenging to meet as new aerodynamic resistances appear with the addition of heat exchangers, shutters, filters and ducts that are multiplied to improve thermal comfort. Recent attempts to optimize this machine have shown the difficulty to improve it while respecting the numerous operating points (ventilation of different areas, heating, air conditioning, defrost, dehumidification), the limited packaging in the dashboard and the constraints of manufacturing. It is furthermore required that the electrical consumption remains at

its lower level, on one hand to improve the energy balance of the vehicle, on the other hand to reduce the on-board mass of electrical motor, wiring, battery and alternator.

The wide diversity of applications, depending on the dashboard characteristics, has lead to the conclusion that blower design should be frequently reconsidered, both for the wheel and the volute if each design has to be optimized. Numerical methods are obviously the key factor to accelerate the development time. In the design strategy presented in this paper, the coupling between an accurate numerical simulation of the blower and an inverse design method is investigated. The strength of the method relies in the ability to quickly predict performances of the proposed geometries and to guide the improvements. The objectives of improving the efficiency, reducing the losses and flow unsteadiness should be reached with a small number of iterations, in a short timeframe.

BLOWER DESCRIPTION

A standard system for Heating and Ventilation Air Conditioning system (HVAC) is presented in Figure 1. The wheel made of plastic has a diameter of about 155 mm. Its maximal rotational speed is limited to 5000 rpm, both for the electrical motor and the acoustics.

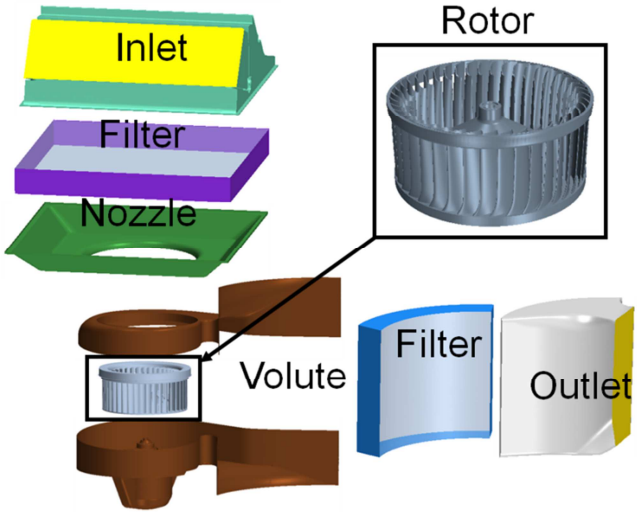

Figure 1: General view of a classical blower for automotive application

Such machine for automotive application is known for the high flow rate delivered regarding the small packaging. This point has triggered numerous investigations with coupled approaches between simulation for flow analysis and experiment for validation, as it was already mentioned and described in [1]. Following the same trend and in order to assess more deeply the ability of simulation to predict complex 3D flow, some campaigns of fine measurement were conducted, as for instance by PIV methods in [2] or by 5 hole probes in [3]. Progress in simulation has allow further studies dealing with unsteadiness and secondary flows in the systems, as for instance in [4] for aerodynamic and in [5] for aeroacoustic purpose. In the same time, analytical and semi-empirical tools have been developed by design engineers to accelerate the design process [6], completed by a physical analysis of root phenomena that have yield some design guidelines [7]. An optimization process based on a Design of Experiment has also been investigated in [8], at the cost of consequent CPU resources.

SIMULATION VALIDATION

An initial study has been conducted to assess the accuracy of the aerodynamic performance prediction. The domain of simulation reproduces the test rig facility located at La Verrière (France), which meets the ISO 5801 requirements [9] for flow and pressure measurements. Great attention has been paid to reproduce accurately the test bench, presented in Figure 2. The domain of

simulation presented in Figure 2 on the right reproduces the blower, its connection to the rig, and the ducted section of the rig equipped with plates to straighten the flow in entrance section. The detailed geometry of the blower is considered since the wheel's hub fixation, the ribs and the gap are included. The recirculation inside the electrical motor is also modelled.

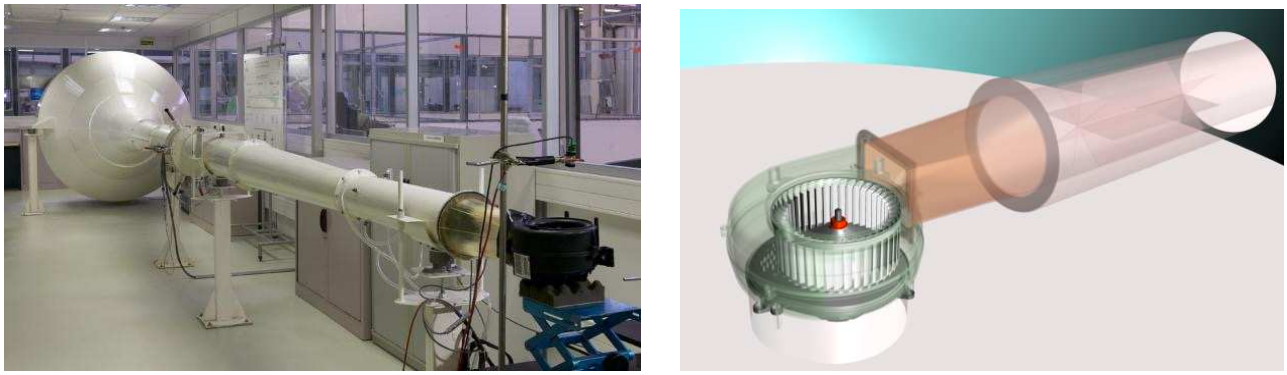

Figure 2

Left: Test rig facility for blowers **Right: Computational domain for the blower**

The numerical simulations have been conducted with the commercial code Star-CCM+ V8.07 from CD-Adapco. The simulation is performed using polyhedra meshes for the two domains that are respectively in rotation for the wheel and at rest for all other components. About 25 millions of polyhedral are used, mainly concentrated in the rotating domain (17 millions) and in the volute (8 millions). In the whole domain of simulation 12 layers of cells are extruded from the surface mesh, yielding to an average wall y+ close to 1 on the wheel and the volute (see Figure 3), and close to 10 elsewhere (motor, test rig). A stagnation total pressure condition is imposed at the inlet, completed with a mass flow at outlet. A steady RANS simulation at the second order with a SST k-ω turbulence model is conducted first to compute the main flow. It is followed by an unsteady RANS simulation (first order on time) which covers several wheel rotations and takes into account the real unsteady behavior of this type of turbomachinery. The convergence of the solution is obtained when residuals drop below 10^{-4} and when the pressure rise and torque become stable over a sufficient period of time. Cycling fluctuations are accepted as long as the average value remains stable during 2 wheel rotations.

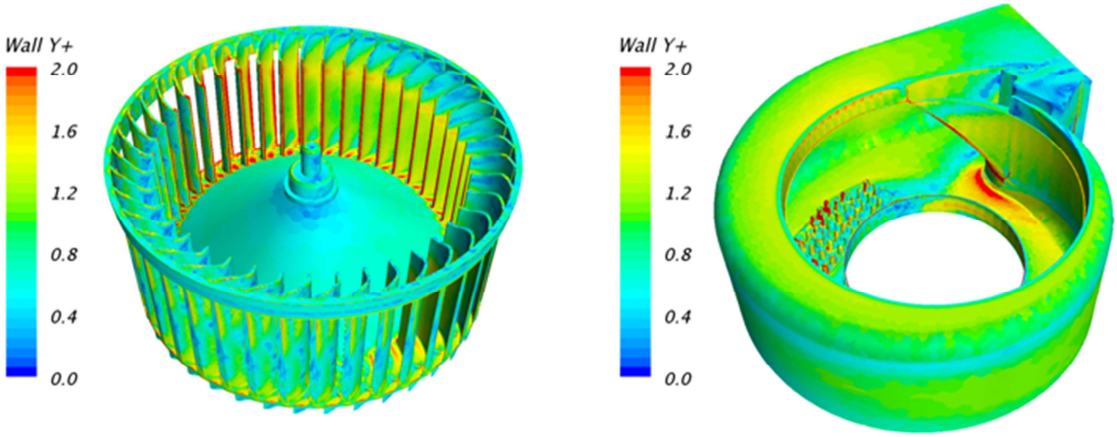

Figure 3: Wheel and volute wall y+ distribution

Global performances are post-processed in term of pressure rise and torque. The static efficiency is deduced from these values. A first comparison between experimental and numerical results is presented in Figure 4. It can be seen that a good agreement is obtained for a large range of flow rate variations. Some slight discrepancies are visible either at low or high flow rate for the steady simulation, but are however strongly reduced when performing an unsteady simulation. Discrepancy analysis is not performed yet, and will be conducted in a specific study equivalent to the one presented in [10] for fan systems. Regarding this previous work, it is expected that error bar on experimental results are about ± 2% on pressure, and ± 5 % on efficiency.

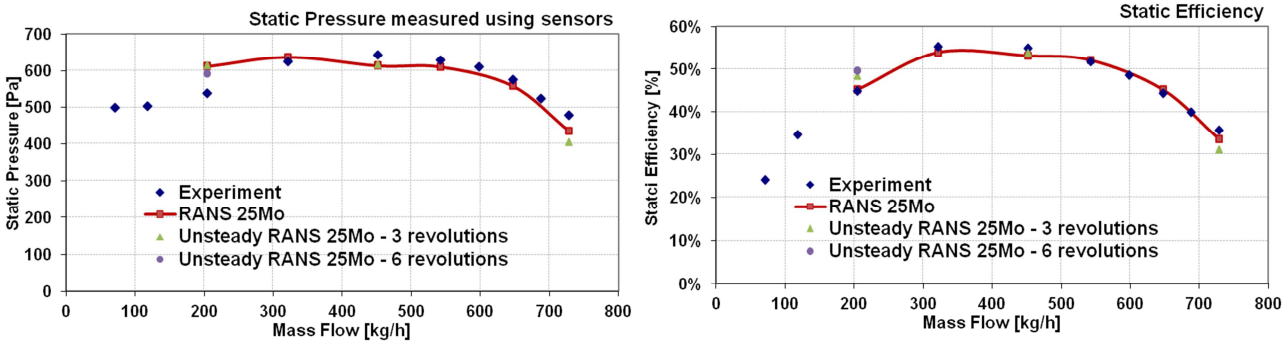

Figure 4: Comparison between experimental and numerical results (static pressure and efficiency)

Further post-processing is presented in Figure 5. A first cut in the domain presents the velocity distribution in the volute: maximum values are of course observed at the wheel exit. These velocities decrease rapidly as the flow fills the scroll, and low flow rate are observed through the electrical motor. The velocity is circumferentially averaged to assess the change in momentum through the wheel by using the (RVt) product. The graph of Figure 5 shows a small amount of pre-swirl at the wheel inlet, in particular close to the bottom (effect of the hub) and close to the tip (effect of the tip clearance). At wheel exit, the curve shows a slightly higher level at bottom as the flow is deflected by the conical hub.

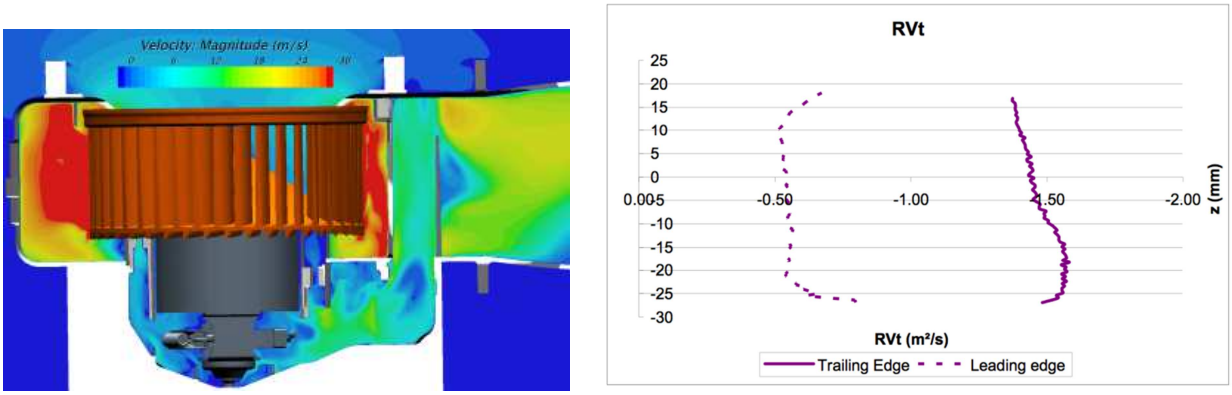

Figure 5: Simulation post-processing

Left: Velocity distribution in a cut plane **Right: RVt distribution along the wheel eight**

INVERSE DESIGN METHOD

TURBOdesign1 [11] has been used to design several type of turbomachinery at Valeo, like the fan presented in [12]. This code uses an inviscid 3D inverse method which computes the blade shape iteratively. To do so, the circumferentially averaged swirl velocity (RVt) has to be prescribed on the meridional channel of the blade, as well as some loading distribution along the chord and

along the spanwise direction. The main input design inputs required by the program are the following:

- A meridional shape for the wheel channel, and for the blade package
- (RVt) distribution at inlet and outlet to specify the workload
- The blade loading distribution along the chord (dRVt/dm).

Several parameters are available to control these inputs and propose different geometries regarding technical choice. Modifications can be driven for instance by the will to decrease loading at tip and bottom, close to the recirculation area created by clearances. In Figure 6, are presented examples of loading distributions as it is imposed in the tool. The code allows for non-free vortex type spanwise RV_θ distribution as well as direct changes to streetwise loading which helps to control the 3D pressure field in the blade directly.

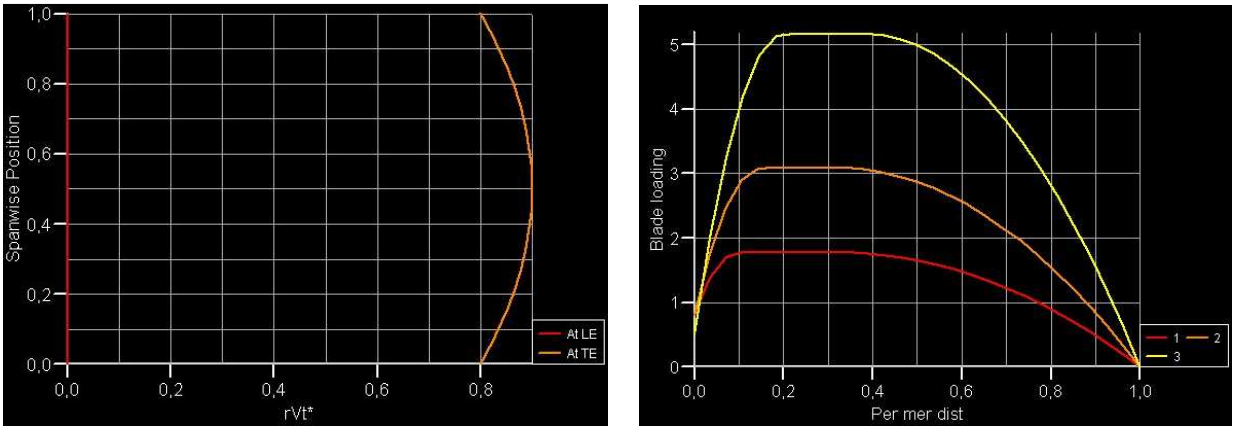

Figure 6: Loading distribution
Left: Along the blade span Right: Along the chord

In a second step, the wheel exit velocity can be used in the volute design code "TURBOdesign Volute" to optimize the volute geometry and its cross section area variation in terms of inlet variation of radial and tangential velocity. The method uses a 2D streamline curvature approach on the volute centerline. It starts with an initial geometry obtained from a 1D method such as conservation of angular momentum approach. The problem is then solved subject to the specified inlet V_r and Vt distribution at inlet to the volute. The mass flow on each quasi-orthogonal is found and this is used to establish the bounding streamline for that section which is then used to define the new volute wall. In this way the volute area variation is established around the circumference. The method can result in quite unconventional area variations that deviate strongly from typical linear variations found in conventional 1D design for this type of volute. In this work the velocity at inlet of volute shown in Figure 7(a) was used to design the volute. This was obtained from the full CFD solution of the baseline stage and using a trendline from the actual variation obtained from CFD. The flow variation around the circumference is highly non-uniform, indicating strong interaction between the impeller and the volute for the blower. In Figure 7(b) the resulting area variation obtained from TURBOdesign Volute using the non-uniform velocities is compared with the results obtained with constant velocity. The volute designed using the inflow variation of velocity (Trendline) results in very large variation in cross section area around the circumference.

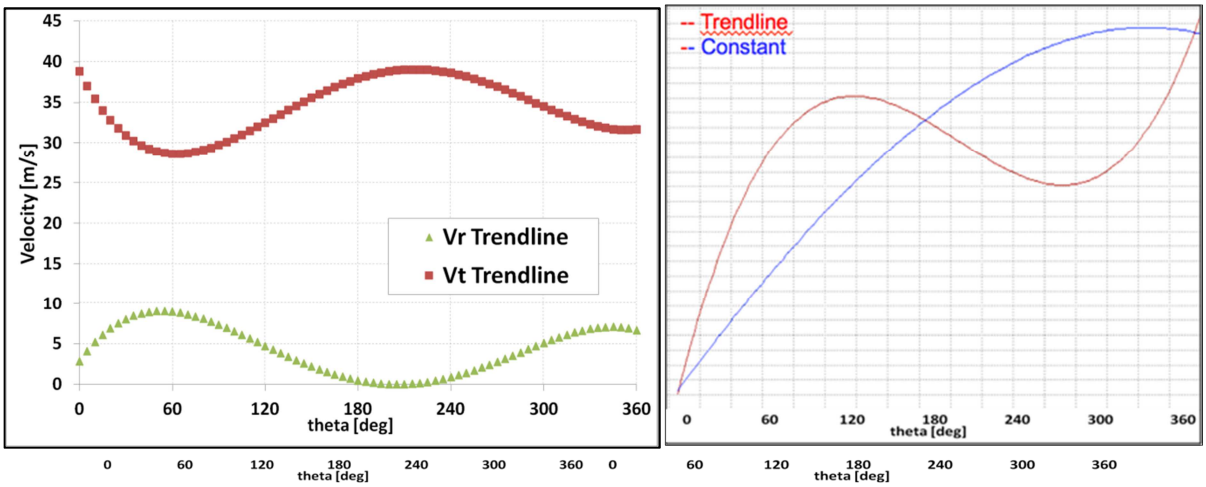

Figure 7: Volute design by 2D inverse design method

a) Specified inlet velocity (trendline) for volute design **b) Resulting area variation for constant velocity and trendline velocity**

Results proposed by these set of tools are rapidly obtained by design engineers once their specifications are analyzed and implemented as inputs of the inverse problem. Direct geometry outputs for both the wheel and the volute allow to quickly connecting these method to the numerical simulation. Figure 8 presents instances of the parts obtained.

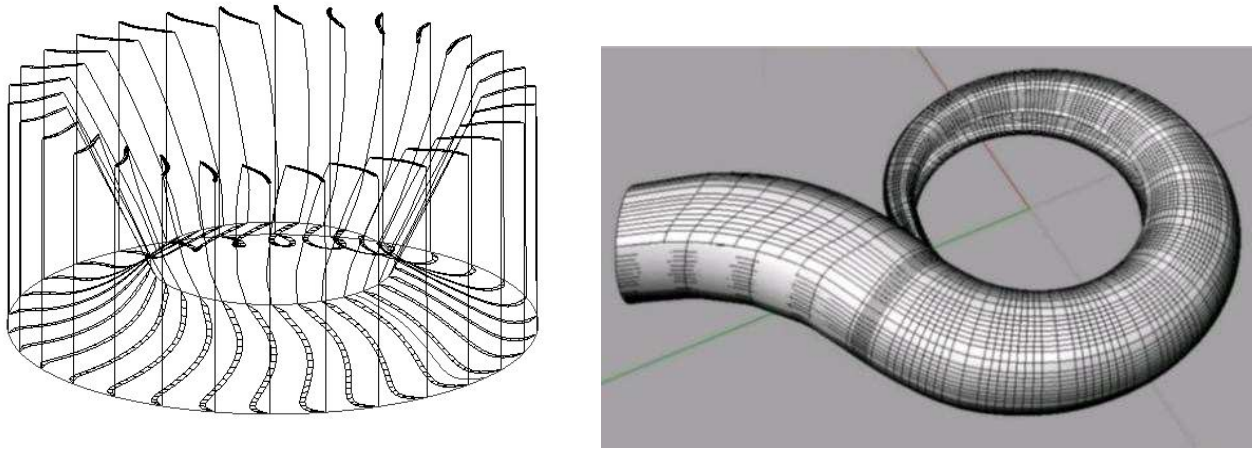

Figure 8: IGES output for geometries

Left: Wheel highly loaded at bottom **Right: Optimized volute**

BLOWER RE-DESIGN AND POST-PROCESSING

A specific simulation set-up was developed to speed-up the turn-over between the design and the performance prediction by CFD. The methodology is to import the IGES format to create a simplified simulation domain, which groups the wheel, the volute and short inlet and outlet domains which contains the filters. The channel for the electrical motor cooling is simplified by using a simple calibrated porous media, allowing thus to keep effect of the recirculation on the performance. The initial conventional design with a squared scroll is presented in Figure 9, and is compared to the newly designed system, which proposes a smoother volute shape with a circular cross-section.

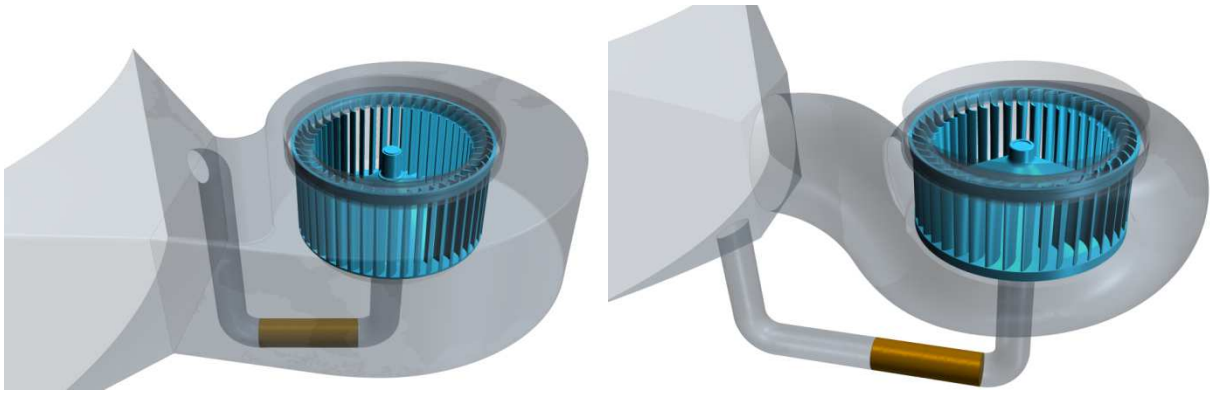

Figure 9: System comparison

Left: Initial with squared volute section **Right: New design with circular volute section**

It must be mentioned that the packaging is quite small, and therefore the wheel has to be highly loaded to achieve the performance. It can be seen on Figure 10 (left), which shows a cut in the blade to blade passage, that the very high angle of attack produces a high level of separation. The high wheel solidity, with a narrow blade to blade passage helps to force the flow radially, and finally it is observed that aerodynamic efficiency and acoustics are quite good (70% static efficiency in our context). All in all, this conventionally designed stage which has been improved continuously over the years offers a good compromise between the packaging, the aerodynamic efficiency and the acoustics. The situation is however greatly improved with the new inverse design rotor design presented in Figure 10 (right). The blade camber has been increased to align better the leading and trailing edge angles to the expected flow deviation. As a result the flow separation region is reduced considerably as compared to the conventional design. However, flow separation is not completely eliminated in the new design as the loading is quite high for such a small wheel, as consequence of the trade-off between aerodynamics and packaging.

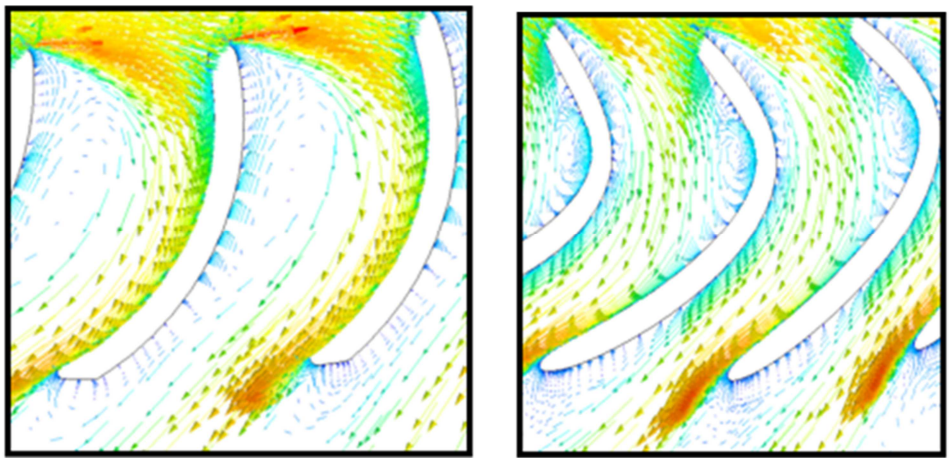

Figure 10: Blade profile comparison with blade to blade flow visualization

Left: Initial (conventional) **Right: New (Inverse) design**

A comparison between flow patterns through the wheels is presented in Figure 11 with vectors for absolute velocities at the exit. A large disturbance close to the volute tongue is clearly observed in Figure 11 (left) for the initial configuration, whereas the newly proposed design shows a much more homogeneous distribution around its circumference. A close look at total pressure distribution inside the system for a cross-section plane at mid span shows an identical advantage for the new

design in terms of homogeneity (Figure 12 right) compared to the initial stage (Figure 12 left). Areas with low values of total pressure are generally smaller with the new inverse designed stage and indicate lower losses.

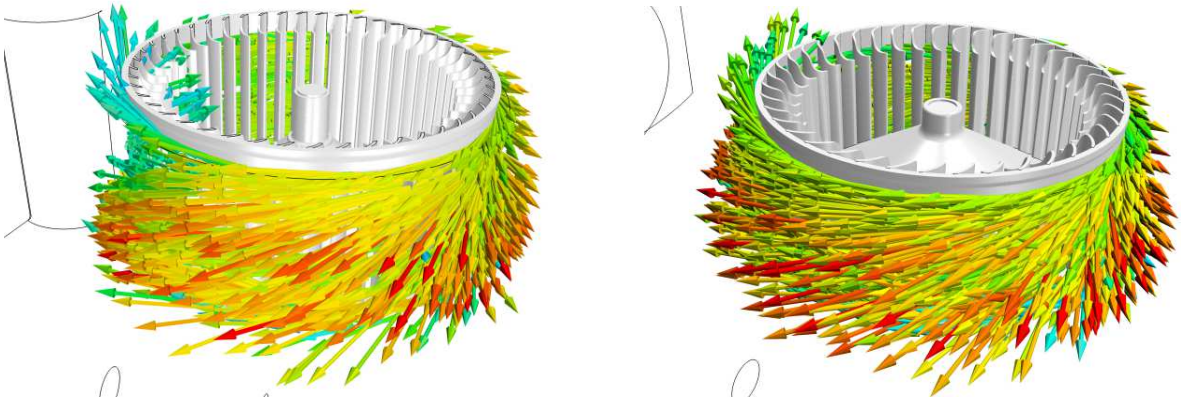

Figure 11: Absolute velocity at wheel outlet

Left: Intial **Right: New design**

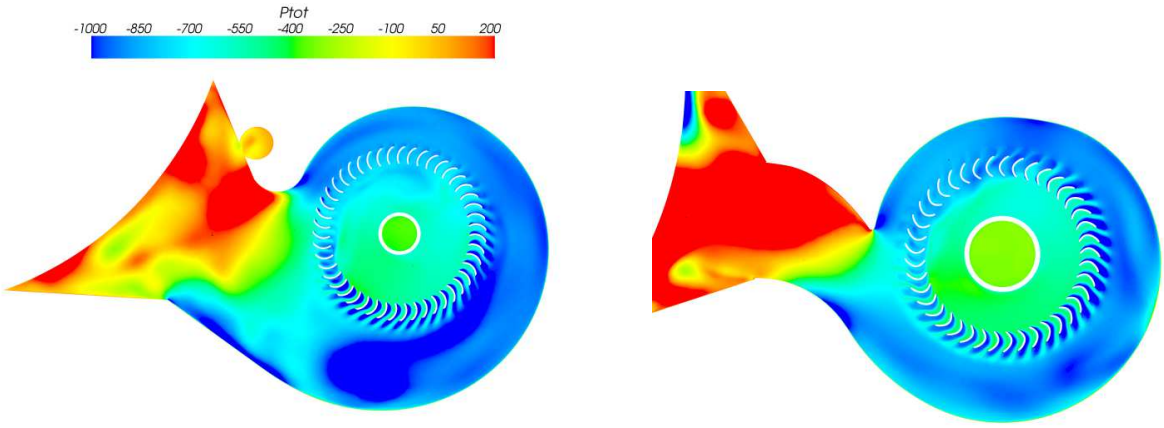

Figure 12: Total pressure at mid span

Left: Initial conventional stage **Right: New inverse designed stage**

An assessment of losses has been made by considering the difference of total pressure between the wheel exit and the scroll exit. The results confirm the improvement as the level of pressure losses is being reduced from 242 Pa to 192 Pa with the re-design. This trend is further confirmed by the analysis of the flow distribution along several cross-sections of volutes, as presented in Figure 13 for the total pressure and Figure 14 for the vorticity. The initial configuration shows large area of losses, mainly concentrated at the wheel bottom where the recirculation from the electrical motor re-enters in the volute. On both side of the volute tongue, i.e for the smaller and the bigger section, the disturbance already detected in Figure 11 is confirmed.

Observations made on Figure 14 for the vorticity magnitude confirm the existence of interactions and high levels of shearing, with a strong evidence of a vortical jet existing from the hub close to the scroll exit. This phenomenon is strongly reduced for the circular volute proposed by the inverse design method. Some traces are obviously present but levels are weaker and the fact it has been almost suppressed close to the tongue is promising for the tonal noise.

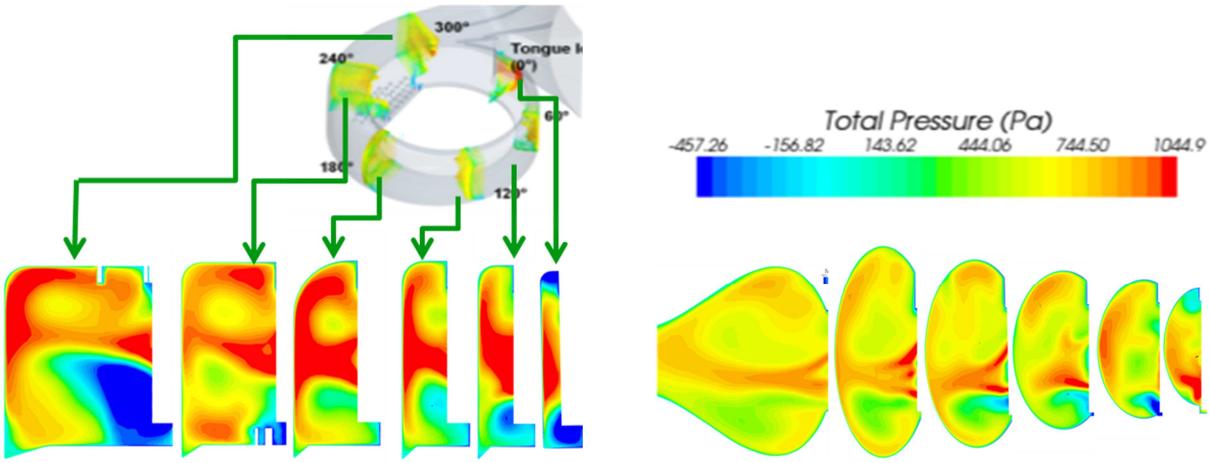

Figure 13: Total pressure along cross-section of the volute

Left: Initial **Right: New design**

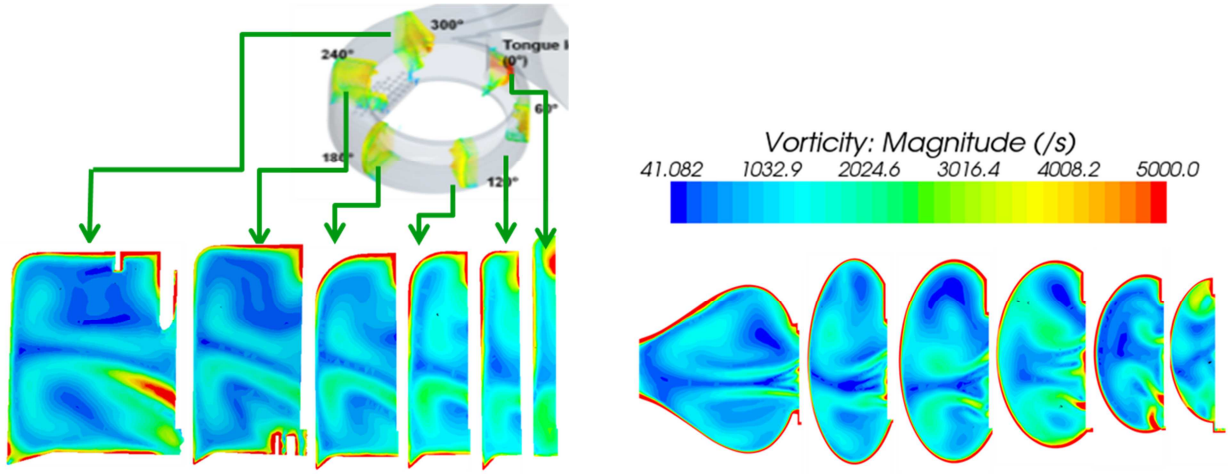

Figure 14: Vorticity magnitude along cross-section of the volute

Left: Initial **Right: New design**

Tonal noise is a frequent issue for automotive blowers since it is unpleasant and subjective noise criteria lead to constraints. The main mechanism producing the tones is coming from the interaction between the tongue, seen as a downstream obstacle, and the blade passing at a constant period. The blade passing frequency of our system is 2392 Hz, a clear and distinct frequency for the human ear. Some investigations are conducted using Power Spectra Density (PSD) from pressure probes located on walls. A relevant position to detect the tonal noise is the head of the volute tongue, on which each wake creates an interaction at the blade passage frequency. Positions of several probes are indicated by red points in the Figure 15 for both the initial and the new system.

The compared PSD presented in this figure show globally lower levels for the new design. For the broadband domain at low frequencies, less dispersion is observed for the new design, and an important gain of about 15 dB is observed. Existence of the tonal peak is of course confirmed for both designs, but the gain is about 10 dB with the circular scroll.

These values should be considered as trends since the noise emitted by the blades themselves is not directly recorded in this approach and no propagation and scattering effects are considered. It is however expected that lower level of unsteadiness is a good indication for acoustic noise reduction.

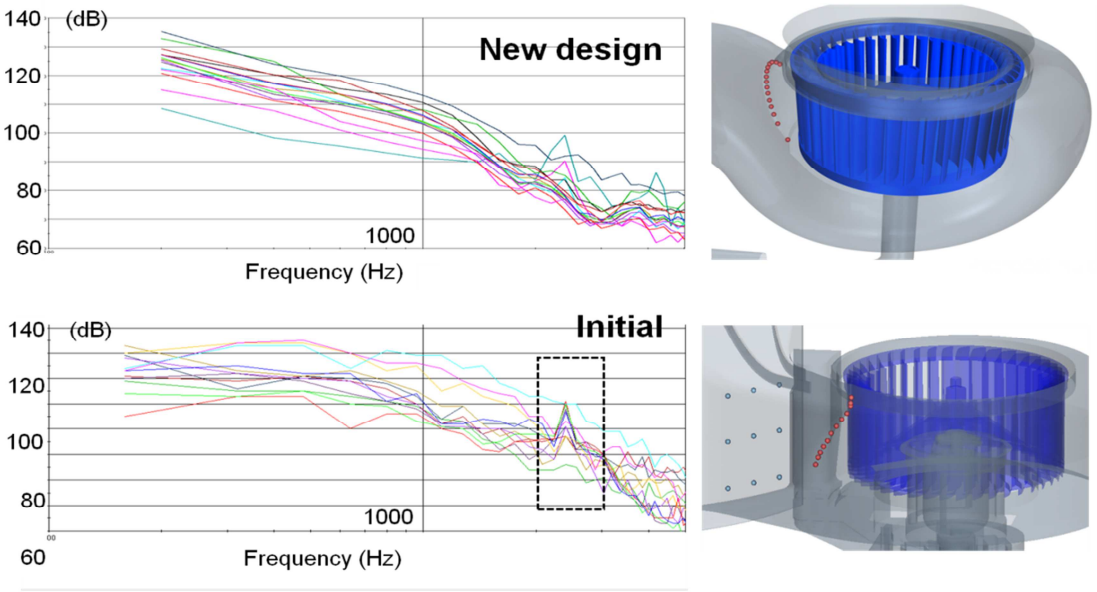

Figure 15: Comparison of PSD on volute tongues

GLOBAL PERFORMANCES

The system analysis has shown some improvements in the flow field within the new blade designed by the 3D inverse design code (less separation) and with the new volute designed by TURBOdesign Volute (less losses). This result is confirmed by the performance prediction at different flow rate, both for the pressure (left figure) and for the efficiency (right figure) of Figure 16.

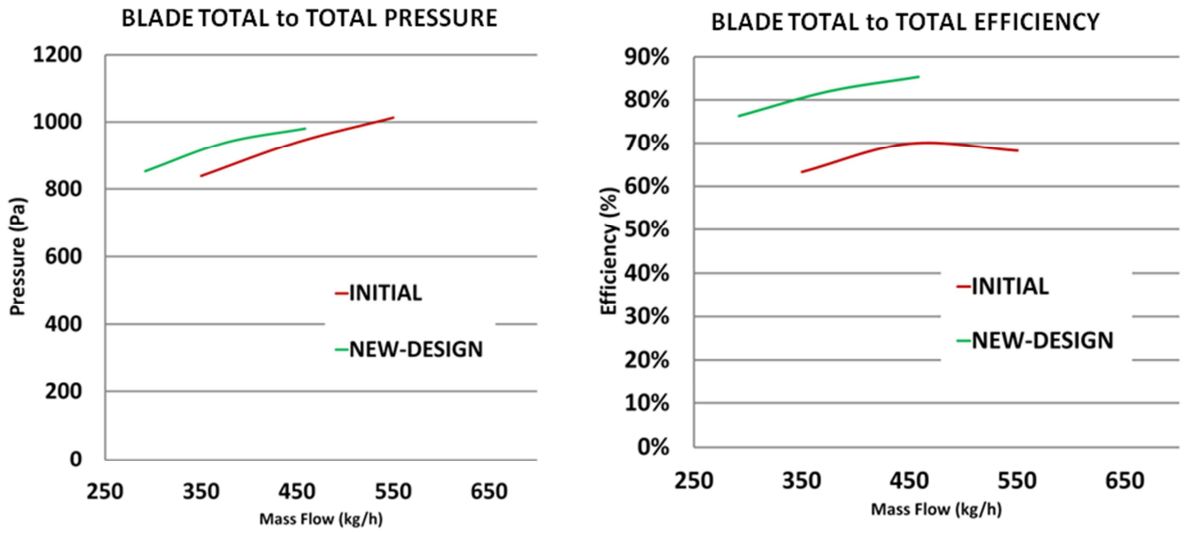

Figure 16: Wheel performance

Left: Total pressure **Right: Total efficiency**

The total to total pressure rise through the wheel is approximately at the same level in both cases, with a slight advantage for the new one. This result was expected as the initial fan performance was used as an input of the inverse design method which produces the second wheel on the base of these specifications. The improvement can be seen on the total to total efficiency which is increased by 10%. This great improvement is obviously obtained thank to the new inverse design blade adapting better to the flow deviation, with a good incidence at leading edge, and being able to camber the

blades to produce the required work without large separation, given the small packaging. System performances are assessed in term of static pressure rise and static efficiency as is the case with our traditional test rig measurement method. The new design shows a more constant head rise behavior which leads to a higher pressure rise at high flow (Figure 16). The heavy space constraints in the system and the resulting under-sized volute have limited performance at high flow rate on the initial design. By redesigning the blower blades and volute, using a novel type of area distribution, the blower efficiency curve has been redistributed without increasing the overall packaging size. This characteristic is obviously beneficial for the cabin comfort with the ability to renew faster air in the cabin. The new stage static pressure rise is slightly lower at low flow rates. However, it must be remarked that the static efficiency is greatly improved over a wide range of flow rates.

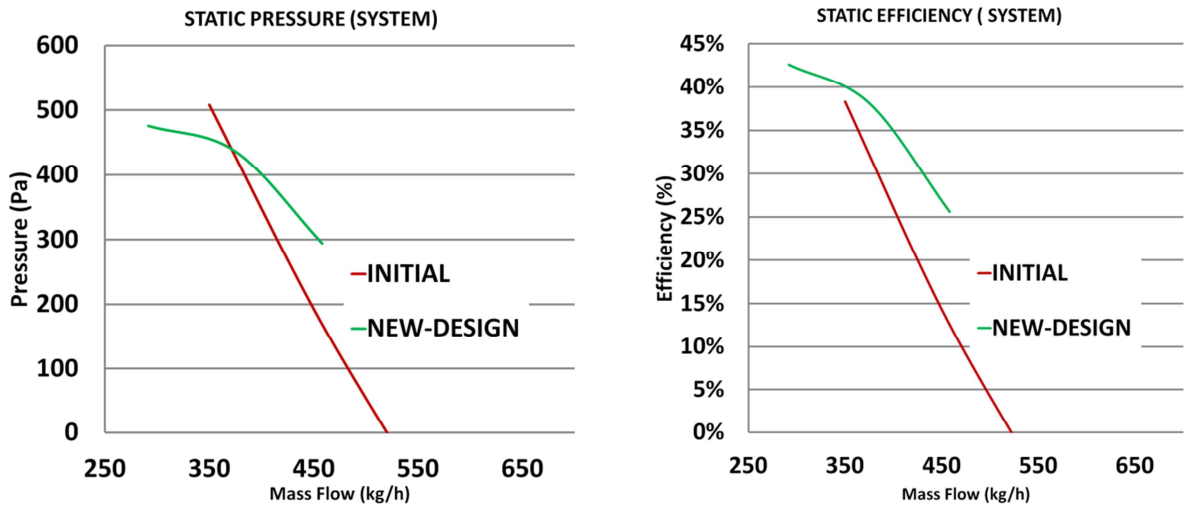

Figure 17: System performance

Left: Pressure rise **Right: Efficiency**

CONCLUSION

Investigations are conducted to define a blower development methodology. It is aimed to take advantage of both the inverse design method, able to produce design in a short time frame, and accurate numerical methods, able to deeply analyze turbomachine behavior.

The design tools used were the 3D inverse design code TURBOdesign1 for rotor blade design and 2D inverse design code TURBOdesign Volute for volute design. The results indicate that the newly designed stage consisting of the new rotor blade and new volute provide significant performance improvements as compared to the initial system. Pressure rise is at the expected level specified by the blade loading, whereas efficiency increases, in particular at high flow rate.

CFD demonstrates the improvement by the flow analysis, which shows a better blade design, less recirculation close to the hub and more efficient flow organization inside the volute. It measures also the level of unsteadiness, in particular close to the tongue where PSD on wall pressure indicates that acoustics should be improved as well.

A long iterative process with CFD may have lead to an equivalent result, however this achievement was obtained in one iteration with a reduced development time and substantial gains on CPU. Coupling the inverse design method and numerical analysis avoids the long development processes commonly observed by engineers using a “trial and error” modification approach. It can lead to exploration of larger design space, novel design solutions and high efficiency at lower development cost.

BIBLIOGRAPHY

[1] "*Design of an Automotive HVAC Blower Wheel for Flow, Noise and Structural Integrity*" Toksoy, C., Zhivov, M., Cutler, F., Ecer, A. et al., SAE Technical Paper 950437, **1995**, doi: 10.4271/950437.

[2] "*Airflow Simulation of an Automotive Blower for a HVAC Unit*" Gronier, P. and Gilotte, P., SAE Technical Paper 960961, **1996**, doi: 10.4271/960961

[3] "*Some Aerodynamic Aspects of Centrifugal Fan Characteristics of an Automotive HVAC Blower"*, Kwon, E., Baek, K., Cho, N., Kim, H. et al., SAE Technical Paper **2001**-01-0291, 2001, doi: 10.4271/2001-01-0291.

[4] "*Numerical and experimental study of unsteady flow in a centrifugal fan*", M. Younsi, F. Bakir, S. Kouidri and R. Rey, Proc. Inst. Mech. Eng., Part A: J. Power Energy, 221(7):1025–1036, **2007**.

[5] "*Unsteady numerical simulations of a low-speed radial fan for aeroacoustics predictions*", M. Sanjosé, S. Moreau, 14th International Symposium on Transport Phenomena and Dynamics of Rotating Machinery, ISROMAC-14, February 27th - March 2nd, **2012**, Honolulu, HI, USA

[6] "*HVAC and battery cooling noises for hybrid / electric vehicles and its impacts on the end user comfort*", Naji S., Ailloud F., SIA, February 4, **2010,** Saint-Ouen – Supméca, France

[7] "*Automotive HVAC unit noise prediction using blower dimensioning tool*", Naji S., Ailloud F., International Conference Automobile and Railroad comfort, Le Mans, France, **2008**, pp. 41-46

[8] "*Automotive blower optimization using parameterized geometries and design of experiment*", M. Henner, B. Demory, P.-A. Bonnet, E. Tannoury, Y. Beddadi, 21st Annual Conference of the CFD Society of Canada, May 6-9, **2013** - Sherbrooke, Quebec CFD Canada

[9] ISO standard DP 5801 – Industrial Fans – performance testing using standardized airways, **1997**.

[10] "*Test Rig Effect on Performance Measurement for Low Loaded Large Diameter Fan for Automotive Application*" M. Henner, B. Demory, F. Franquelin, Y. Beddadi, Z. Zhang, ASME Turbo Expo **2014**, Paper No. GT2014-27071, pp. V01AT10A031; 11 pages doi: 10.1115/GT2014-27071

[11] "*On the Coupling of Inverse Design and Optimization Techniques for the Multiobjective, Multipoint, Design of Turbomachinery Blades*", Bonaiuti D., Zangeneh M., Transactions of the ASME, 021014-16 / Vol. 131, April, **2009**.

[12] "*Low weight, high speed automotive fan design by 3D inverse method*", M. Henner, B. Demory, Y. Beddadi, P.A. Bonnet, F. Pengue, M. Zangeneh, European Turbomachinery Conference, (ETC10), 15-19 April, **2013**, Lappeenranta, Finland.